

Novel two-directional grid multi-scroll chaotic attractors based on the Jerk system

Peng-Fei Ding(丁鹏飞)^{1,2}, Xiao-Yi Feng(冯晓毅)^{1,†}, and Cheng-Mao Wu(吴成茂)²

¹School of Electronics and Information, Northwestern Polytechnical University, Xi'an 710072, China

²School of Electronics and Engineering, Xi'an University of Posts and Telecommunications, Xi'an 710121, China

(Received 19 April 2020; revised manuscript received 14 June 2020; accepted manuscript online 18 June 2020)

A new method is presented to generate two-directional (2D) grid multi-scroll chaotic attractors via a specific form of the sine function and sign function series, which are applied to increase saddle points of index 2. The scroll number in the x -direction is modified easily through changing the thresholds of the specific form of the sine function, while the scroll number in the y -direction is controlled by the sign function series. Some basic dynamical properties, such as equilibrium points, bifurcation diagram, phase portraits, and Lyapunov exponents spectrum are studied. Furthermore, the electronic circuit of the system is designed and its simulation results are given by Multisim 10.

Keywords: grid multi-scroll chaotic attractor, Jerk system, specific form of the sine function, circuit implementation

PACS: 82.40.Bj, 05.45.Pq, 05.45.–a

DOI: 10.1088/1674-1056/ab9dea

1. Introduction

It is well known that the chaotic system has the characteristics of sensitivity of initial value and complexity of trajectory, so chaos has great potential application in many engineering fields, such as weak signal detection,^[1–4] random number generator,^[5,6] secure communication,^[7–13] and image encryption.^[14–20] Furthermore, Lin *et al.*^[21,22] studied the influence of electromagnetic radiation on the chaotic characteristics of neural networks, and found that appropriate electromagnetic radiation is helpful to treat some neurological diseases. Since memristor has the characteristics of nonlinear and memory, Yu *et al.*^[23–26] proposed some hyperchaotic systems based on memristor. On the circuit realization of the chaos system, Yu *et al.*^[27] completed the circuit implementation of a multistable modified fourth-order autonomy Chua's chaos system based on second-generation current conveyors (CCII) and field programmable gate array (FPGA).

Since multi-scroll chaotic attractors were proposed by Suykens in 1993,^[28] one-directional (1D) n -scroll,^[28–36] two-directional (2D) $n \times m$ grid scroll,^[32,33,35,37] and three-directional (3D) $n \times m \times l$ -grid scroll^[33–35] chaotic attractors have been designed. In addition to the multi-scroll chaotic system, the multi-wing chaotic system has also been studied.^[38] Li *et al.*^[39] constructed a new three-dimensional autonomous chaotic system. Zhang *et al.*^[40] introduced a new chaotic system with bond orbital attractors, and indicated that the chaotic attractors can be divided into self-excited attractor and hidden attractor. Zhang *et al.* proposed a multi-scroll hyperchaotic system with hidden attractors^[41] and a self-excited attractor multi-scroll chaotic system.^[42] Deng *et al.*^[43] gave an example of multi-scroll hidden attractors. Ji *et al.*^[44] pro-

posed a modified mathematical model for intracellular Ca^{2+} oscillations and studied its bifurcation behavior, Nguyen *et al.*^[45] studied the effect of temperature variation on the output dynamics of a carbon nanotube field-effect transistor (CN-FET) based chaotic generator. Yasuomi^[46] studied how the temperature affects the frequency–current (f – I) curve and phase response curve (PRC) of the neural oscillation. Zhou *et al.*^[47] analyzed the effect of temperature on a two-phase clock-driven discrete-time chaotic circuit. Nam *et al.*^[48] and Nguyen *et al.*^[49] proposed chaotic oscillators based on photodiode. Li *et al.*^[50] discovered the bifurcation mechanism of bursting oscillation with two slow variables. Niu *et al.*^[51] showed that Bcl-2 has a crucial role in the oscillatory region of Ca^{2+} signaling through two-parameter bifurcation analyses. Zhang *et al.*^[52] proposed a novel secure key distribution scheme based on the unidirectional injection of the vertical cavity surface emitting laser (VCSEL) system. Li *et al.*^[53] presented an algorithm for computing 2D stable and unstable manifolds of hyperbolic fixed points of nonlinear maps, and its performance was demonstrated by hyperchaotic 3D Hénon map and Lorenz system. Zhang *et al.*^[54] and Han *et al.*^[55] discussed the dynamical behaviors of bursting oscillations. Zhang *et al.*^[56] studied the existence and stability of the Hopf bifurcation of a modified Pan-like chaotic system. Wang *et al.*^[57] discovered that the concentration of p53 can show oscillations with short or long periods upon DNA damage, and the results suggest that p53 birhythmicity enhances the responsiveness of the p53 network, which may facilitate its tumor-suppressive function. Gao *et al.*^[58] analyzed the internal effects of the dynamic behaviors and nonlinear characteristics of a coupled fractional-order hydropower genera-

[†]Corresponding author. E-mail: fengxiao@nwpu.edu.cn

tion system (HGS). Dong *et al.*^[59,60] studied the stable target patterns and the defects in the transition from square to square grid states in dielectric barrier discharge, which provides a reference for the chaos system in defect detection. Nonlinear function is the key to generate scroll in autonomous chaotic system, and the applied nonlinear functions are piecewise linear function,^[28,29,32] sign function,^[30,31,33,61,62] triangular wave,^[31,63] saw-tooth wave,^[31] saturated function,^[31,35] hysteresis function,^[31] and so on.

In the 3D differential equation, the general Jerk system has fewer terms, so the chaotic system based on the general Jerk system has been extensively studied.^[35,64–70] The number of scrolls in multi-scroll chaotic attractors is related to the number of equilibrium points. For generating a fixed number of scrolls, many researchers limit the number of equilibrium points by changing the expression of sine function or using negative feedback.^[64,67,70–76] Ma *et al.*^[67] used negative feedback to limiting the range of the state variable, and the number of scrolls was determined. Yu *et al.*^[70] controlled the number of scrolls by a modulated sine function, and Tang *et al.*^[71] proposed an approach to generate a fixed number of scrolls in a chaotic system with the modified sine function, which consists of three segments: the middle segment is a sine function, while the other two segments are the first-order functions. As mentioned in the above reference, the number of scrolls with a non-modified sine function is varied with the simulation time, meanwhile, the modified sine functions^[70,71] are complex and the circuit implementation is sophisticated. Furthermore, to our best knowledge, the chaotic system based on sine function generates scrolls only in one direction. Therefore, it is very interesting to ask whether or not there is a simpler modified sine function that can generate 2D chaotic attractors? This paper gives an affirmative answer to this question. More exactly, this paper gives a simple modified sine function approach to generate 2D chaotic system based on general Jerk system and the circuit diagram is designed for circuit realization of the 2D chaotic system.

Compare with other 2D grid multi-scroll chaotic system, the most important feature of our proposed chaotic system is to use a special form of sine function for generating scrolls in the x -direction, and the system has the following advantages. (i) The number of the used electronic components in circuit realization is independent of the number of scrolls in the x -direction. (ii) The hardware circuits of the special form of the sine function generator for generating scrolls in the x -direction only need three operational amplifiers, three reference voltages, and one analog multiplier. (iii) The scroll numbers of the system in the left and right parts of the x -direction can be arbitrarily adjusted by changing only two comparison voltages of the special form of the sine function generator.

The rest of the paper is organized as follows. In Section 2, a one-directional (1D) multi-scroll chaotic system is intro-

duced based on a sine function and general Jerk system, then a 2D multi-scroll chaotic system is designed and the phase portraits of the system are given. In Section 3, we study and analyze the dynamical properties and behaviors of the designed chaotic system, including the calculation of equilibrium points and numerical simulation for bifurcation. In Section 4, circuit implementations of the 2D multi-scroll chaotic system are investigated, and the simulation result indicates the feasibility of the circuit implementation. Finally, the conclusions are drawn in Section 5.

2. A novel 2D chaotic system based on the Jerk system

The general Jerk system is described by

$$x + \beta \ddot{x} + \gamma \dot{x} = f(x), \quad (1)$$

where x is the displacement, \dot{x} is the derivative of the displacement called velocity, \ddot{x} is the derivative of the velocity called acceleration, and $\dot{\ddot{x}}$ is the derivative of the acceleration called Jerk. Taking $y = \dot{x}$ and $z = \dot{y}$, equation (1) can be rewritten as follows:

$$\begin{cases} \dot{x} = y, \\ \dot{y} = z, \\ \dot{z} = -\gamma y - \beta z + f(x). \end{cases} \quad (2)$$

Based on Eq. (2), a novel 1D multi-scroll chaotic system is proposed as follows:

$$\begin{cases} \dot{x} = y, \\ \dot{y} = z, \\ \dot{z} = -ay - cz - df(x), \end{cases} \quad (3)$$

where

$$f(x) = \begin{cases} -\sin(2\pi bx), & -n_1/b < x < n_2/b, \\ +\sin(2\pi bx), & x \leq -n_1/b, \\ +\sin(2\pi bx), & x \geq n_2/b. \end{cases} \quad (4)$$

It should be noticed that $f(x)$ is a specific form of the sine function, which is different from the sine function $g(x)$,^[64,67,74–76] the modulating sine function $h(x)$,^[70] the modified sine function $p(x)$,^[71]

$$g(x) = \sin(2\pi bx), \quad (5)$$

$$h(x) = |A \sin(ax)| \operatorname{sgn}(x) - x, \quad (6)$$

$$p(x) = \begin{cases} \frac{b\pi}{2a}(x - 2ac), & x \geq 2ac, \\ -b \sin\left(\frac{\pi x}{2a} + d\right), & -2ac < x < 2ac, \\ \frac{b\pi}{2a}(x + 2ac), & x \leq -2ac. \end{cases} \quad (7)$$

The waveforms of the sine functions $f(x)$, $g(x)$, $h(x)$, and $p(x)$ are depicted in Fig. 1.

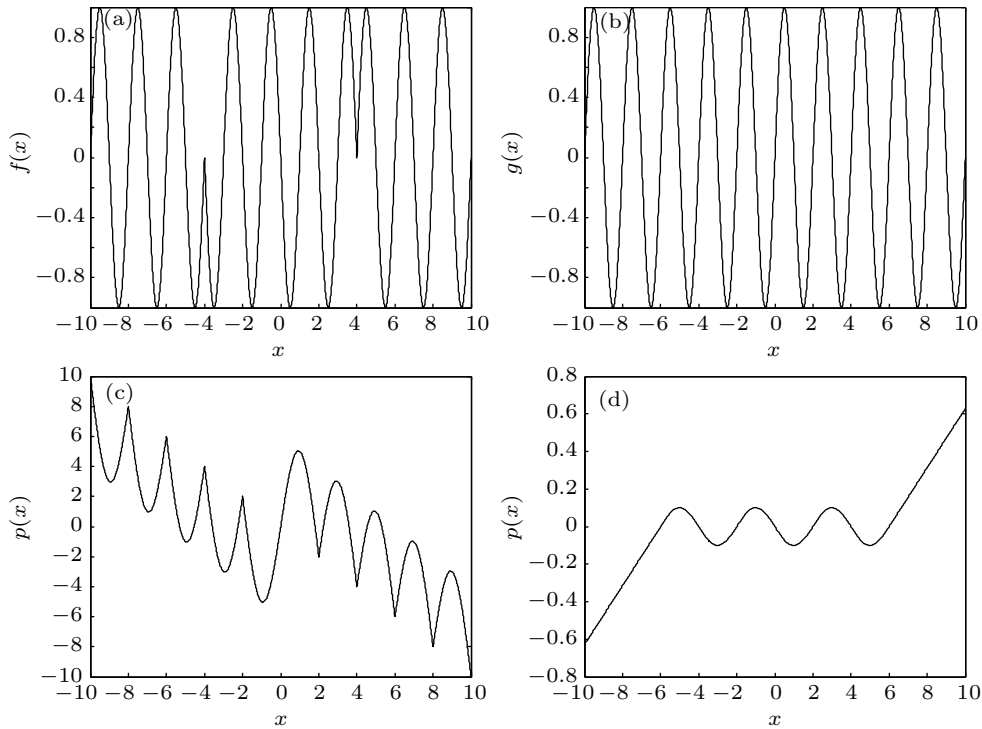


Fig. 1. The waveform of the different sine functions: (a) $f(x)$ with $b = 0.5$ and $n_1 = n_2 = 2$, (b) $g(x)$ with $b = 0.5$, (c) $h(x)$ with $A = 6$ and $a = 0.5\pi$, (d) $p(x)$ with $a = 1$, $b = 0.1$, $c = 3$, and $d = 0$. The a, c , and d are real constants, and x, y , and z are state variables of the system (3). The b, n_1 , and n_2 are real constants in Eq. (4). The number of scrolls generated by the system (3) with suitable parameters can be adjusted by the parameters n_1 and n_2 .

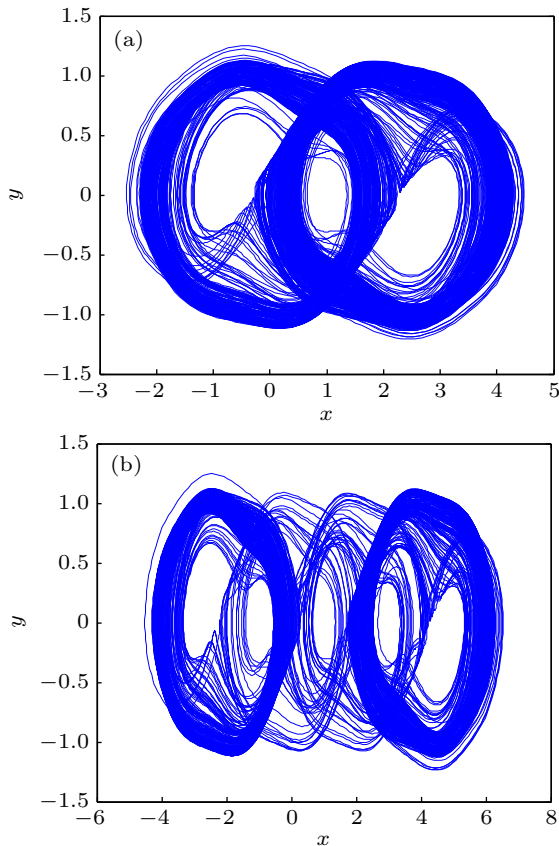


Fig. 2. Different number of scroll chaotic attractors are generated by system (3) with $a = c = d = 0.3$ and $b = 0.5$: (a) 3-scroll chaotic attractor with $n_1 = 1$ and $n_2 = 2$, (b) 5-scroll chaotic attractor with $n_1 = 2$ and $n_2 = 3$.

The multi-scroll chaotic attractor can be observed when

the parameters a, b, c , and d are in the chaotic region. When the parameters are selected as $a = c = d = 0.3$ and $b = 0.5$, system (3) with different values of n_1 and n_2 can generate different numbers of scroll chaotic attractors. Taking $n_1 = 1, n_2 = 2$ and $n_1 = 2, n_2 = 3$ as examples, the simulation results of 3-scroll and 5-scroll chaotic attractors are shown in Fig. 2.

From Fig. 2, it can be concluded that system (3) with Eq. (4) can generate 1D multi-scroll chaotic attractors, and the number of scrolls is determined by n_1 and n_2 , the scroll number M is given by

$$M = n_1 + n_2. \tag{8}$$

For generating $m \times n$ -scroll chaotic attractors, we extend the scrolls to y -direction by using a step function series $f_1(y)$ into system (3), that is,

$$\begin{cases} \dot{x} = y - f_1(y), \\ \dot{y} = z, \\ \dot{z} = -a(y - f_1(y)) - cz - df(x), \end{cases} \tag{9}$$

where

$$f_1(y) = A \left[\sum_{i=0}^{M-1} (\text{sign}(y + (2i + 1)A) + \text{sign}(y - (2i + 1)A)) \right], \tag{10}$$

or

$$f_1(y) = A \left[-\text{sign}(y) + \sum_{i=0}^{M-1} (\text{sign}(y + (2i)A) + \text{sign}(y - (2i)A)) \right]. \tag{11}$$

Equations (10) and (11) are for generating $2M + 1$ -scroll and $2M$ -scroll chaotic attractors in the y -direction, respectively. In Eqs. (10) and (11), $A > 0$ and M is a non-negative integer, $\text{sign}(y)$ is a signal function, which is given as

$$\text{sign}(y) = \begin{cases} 1, & y > 0, \\ 0, & y = 0, \\ -1, & y < 0. \end{cases} \quad (12)$$

According to Eqs. (4) and (9)–(12), system (9) can generate $m \times n$ -scroll chaotic attractors. For example, setting $n_1 = 3$, $n_2 = 3$, $A = 1$, $M = 1$, and $f_1(y)$ is selected as Eq. (10), the chaotic system (9) can generate 6×3 grid multi-scroll attractors, while setting $n_1 = 2$, $n_2 = 3$, $A = 1$, $M = 2$, and $f_1(y)$ is selected as Eq. (11), the chaotic system (9) can generate 5×4 grid multi-scroll attractors. The simulation results of the grid multi-scroll attractors with $a = 1, b = 0.5, c = 0.3, d = 0.5$ and initial values $(0.1, 0.1, 0.1)$ are shown in Fig. 3.

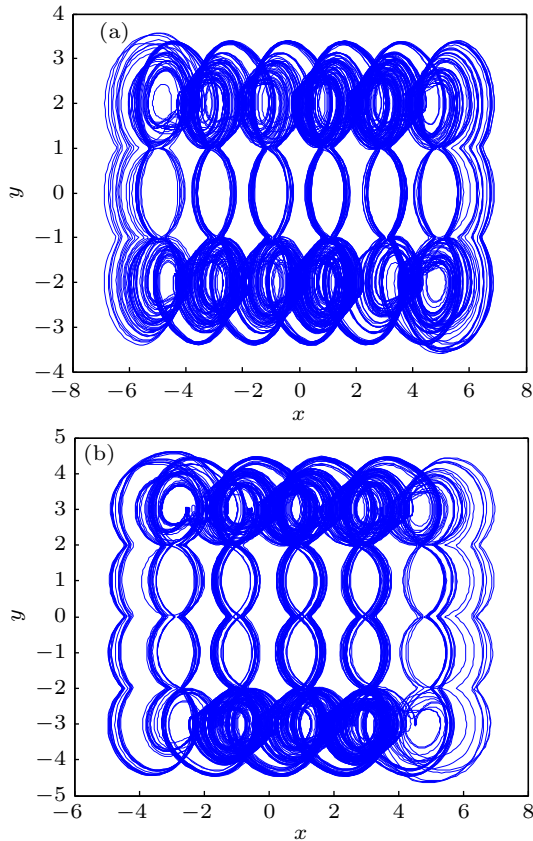


Fig. 3. Grid multi-scroll chaotic attractors for $a = 1, b = 0.5, c = 0.3, d = 0.5$, and $A = 1$: (a) 6×3 grid multi-scroll chaotic attractors with $n_1 = 3, n_2 = 3$, and $M = 1$; (b) 5×4 grid multi-scroll chaotic attractors with $n_1 = 2, n_2 = 3$, and $M = 2$.

3. Theoretical analysis of the novel chaotic system

In this section, the dynamical characteristics of the novel chaotic system (9), such as equilibrium points, Lyapunov exponents, and bifurcation diagram are studied.

3.1. Equilibrium points

In order to obtain the equilibrium points of system (9), let the right hand side of system (9) equal to zero, then

$$\begin{cases} y - f_1(y) = 0, \\ z = 0, \\ a(y - f_1(y)) + cz + df(x) = 0. \end{cases} \quad (13)$$

In Eq. (13), $f_1(y)$ is selected as Eq. (10) to study the equilibrium points, and the equilibrium points of the system (9) are $E_1(x_1^*, y_1^*, 0), E_2(x_2^*, y_1^*, 0), E_3(x_1^*, y_2^*, 0)$, and $E_4(x_2^*, y_2^*, 0)$, where

$$x_1^* = (2i+1)/2b, \quad i \in \{-n_1-1, -n_1, \dots, -1, 0, 1, \dots, n_2\}; \quad (14)$$

$$x_2^* = i/b, \quad i \in \{-n_1, \dots, -1, 0, 1, \dots, n_2\}; \quad (15)$$

$$y_1^* = \pm 2iA, \quad i \in \{0, 1, 2, \dots, M\}; \quad (16)$$

$$y_2^* = \pm(2i+1)A, \quad i \in \{0, 1, 2, \dots, M-1\}. \quad (17)$$

By linearizing system (9), the Jacobian matrix can be expressed as

$$J = \begin{pmatrix} 0 & 1 - f_1'(y) & 0 \\ 0 & 0 & 1 \\ -df'(x) & -a(1 - f_1'(y)) & -c \end{pmatrix}. \quad (18)$$

Take the 6×3 grid multi-scroll as an example and the parameter values are set as above mentioned. For equilibrium points $E_1(x_1^*, y_1^*, 0)$, the corresponding characteristic equation is

$$\lambda^3 + c\lambda^2 + a\lambda + d\pi = \lambda^3 + 0.3\lambda^2 + \lambda + 0.5\pi = 0. \quad (19)$$

The solutions of Eq. (19) are $\lambda_1 = -0.9608, \lambda_{2,3} = 0.3304 \pm 1.2352i$. Equation (19) has one negative root and a pair of complex conjugate roots with positive real parts. Thus the equilibrium points $E_1(x_1^*, y_1^*, 0)$ are saddle points of index 2.

For equilibrium points $E_2(x_2^*, y_1^*, 0)$, the corresponding characteristic equation is

$$\lambda^3 + c\lambda^2 + a\lambda - d\pi = \lambda^3 + 0.3\lambda^2 + \lambda - 0.5\pi = 0. \quad (20)$$

The solutions of Eq. (20) are $\lambda_1 = 0.8193, \lambda_{2,3} = -0.5579 \pm 1.2665i$. Equation (20) has one positive root and a pair of complex conjugate roots with negative real parts. Thus the equilibrium points $E_2(x_2^*, y_1^*, 0)$ are saddle points of index 1.

For equilibrium points $E_3(x_1^*, y_2^*, 0)$, the corresponding characteristic equation is

$$\lambda^3 + 0.3\lambda^2 + (1 - f_1'(y_2^*))\lambda + 0.5\pi(1 - f_1'(y_2^*)) = 0. \quad (21)$$

At equilibrium points $E_3(x_1^*, y_2^*, 0)$, equation (21) has one positive root and two negative roots. That is, the equilibrium points $E_3(x_1^*, y_2^*, 0)$ are saddle points of index 1.

For equilibrium points $E_4(x_2^*, y_2^*, 0)$, the corresponding characteristic equation is

$$\lambda^3 + 0.3\lambda^2 + (1 - f_1'(y_2^*))\lambda - 0.5\pi(1 - f_1'(y_2^*)) = 0. \quad (22)$$

At equilibrium points $E_4(x_2^*, y_2^*, 0)$, the equation (22) has one negative root and two positive roots. That is, the equilibrium points $E_4(x_2^*, y_2^*, 0)$ are saddle points of index 2.

The distribution of equilibrium points is shown in Fig. 4, and the equilibrium points $E_1, E_2, E_3,$ and E_4 are marked with $*, \circ, \Delta, \square,$ respectively. From Figs. 4 and 3(a), it can be seen that the scrolls are generated only around the equilibrium points E_1 , which are saddle points of index 2.

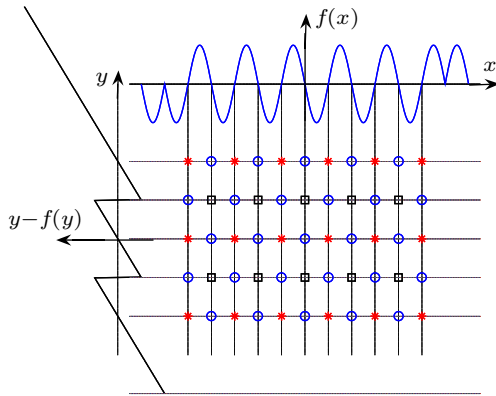


Fig. 4. The equilibrium point distribution of the 6×3 grid multi-scroll chaotic attractors.

3.2. Lyapunov exponents and bifurcation diagram

For dynamical system (9) with Eqs. (4) and (10), and parameters are selected as $a = 1, b = 0.5, c = 0.3, n_1 = n_2 = 3,$ and $M = 1,$ the Lyapunov exponent spectrum with $d \in (0, 1)$ is displayed in Fig. 5(a), and the corresponding bifurcation diagram is shown in Fig. 5(b). In this paper, we always assume that the Lyapunov exponents satisfy $LE_1 \geq LE_2 \geq LE_3,$ then dynamical characteristic of

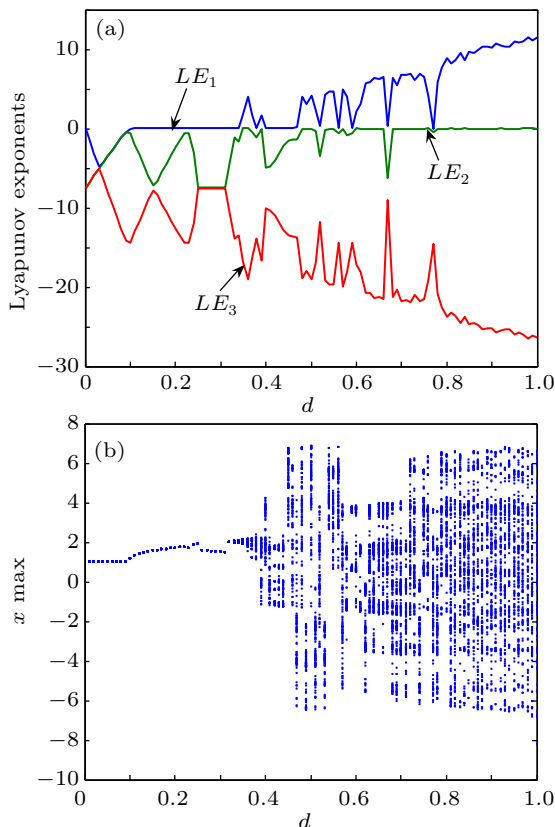


Fig. 5. The system (9) with Eqs. (4) and (10), and $d \in (0, 1)$: (a) Lyapunov exponents; (b) bifurcation diagram.

system (9) in the interval $d \in (0, 1)$ is summarized as follows:

1. when $d \in (0, 0.1], LE_1 < 0, LE_2 < 0, LE_3 < 0,$ the system (9) is stable;
2. when $d \in (0.1, 0.34] \cup [0.4, 0.46], LE_1 = 0, LE_2 < 0, LE_3 < 0,$ the system (9) is periodic;
3. when $d \in (0.34, 0.4] \cup (0.46, 1), LE_1 > 0, LE_2 = 0, LE_3 < 0,$ the system (9) is chaotic.

When $a = 1, b = 0.5, c = 0.3, d = 0.5, n_1 = 3, n_2 = 3,$ and $f_1(y)$ is selected as Eq. (10) with $A = 1, M = 1,$ the 6×3 grid multi-scroll chaotic attractors are shown in Fig. 3(a), and their Lyapunov exponents are $LE_1 = 4.1565, LE_2 = -0.0109, LE_3 = -19.0488$ for initial values $(0.1, 0.1, 0.1),$ and the Lyapunov dimension is $D_{LE} = 2.2176,$ which is calculated by

$$D_{LE} = j + \frac{1}{|LE_{j+1}|} \sum_{i=1}^j LE_i. \quad (23)$$

In Eq. (23), j is the largest integer which satisfies $\sum_{i=1}^j LE_i > 0$ and $\sum_{i=1}^{j+1} LE_i < 0.$ Thus, the 6×3 grid multi-scroll chaotic attractors are fractional.

4. Grid multi-scroll circuit implementation on Multisim10

In this section, electronic circuits are implemented on Multisim10 to confirm that system (9) can generate multi-scroll chaotic attractors. Firstly, the specific form of the sine function circuit is designed according to Eq. (4). Secondly, the two kinds of step function series are designed along with Eqs. (10) and (11), respectively. Lastly, the electronic circuits for the 6×3 and 5×4 grid multi-scroll chaotic attractors are designed, and the simulation results on Multisim10 are given.

4.1. Circuit design for the specific form of the sine function generator

According to Eq. (4), the electronic circuit for sine function $f(x)$ with $b = 0.5, n_1 = n_2 = 3$ is designed, and the circuit diagram and simulation result are shown in Fig. 6. In Fig. 6, the unit of horizontal ordinate is 2 s/Div, while the unit of vertical ordinate is 500 mV/Div.

The electronic circuit for sine function $f(x)$ with $b = 0.5, n_1 = n_2 = 2$ is designed as Fig. 7(a), and the simulation result is shown in Fig. 7(b). The unit of horizontal ordinate in Fig. 7(b) is 2 s/Div, while the unit of vertical ordinate is 500 mV/Div.

In Figs. 6 and 7, the supply power for operational amplifier uA741 is ± 15 V, and the saturation voltage of uA741 is ± 13.5 V with the supply voltage equaling ± 15 V. The selection of resistance satisfies $R_3/R_2 = R_1/R_2 = 1/13.5, R_3/R_4 = 1, R_1 = R_2 = 27$ k $\Omega,$ and $R_3 = R_4 = 2$ k $\Omega.$ v_a and v_b in Figs. 6 and 7 represent n_2/b and $-n_1/b,$ respectively, where n_1 is the number of scrolls in the negative part of the x -axis and n_2 is the number of scrolls in the positive part of the x -axis. Furthermore, b represents the frequency of the specific form of sine function $f(x).$ In Fig. 6, we set the frequency of the sine

function $f(x)$ as 0.5 Hz and $v_a = 6\text{ V}$ and $v_b = -6\text{ V}$, then $n_1 = n_2 = 3$. In Fig. 7, we set the frequency of the sine function $f(x)$ as 0.5 Hz, $v_a = 6\text{ V}$ and $v_b = -4\text{ V}$, then $n_1 = 2$ and $n_2 = 3$. It should be pointed out that the values of n_1 and n_2 can be set arbitrarily.

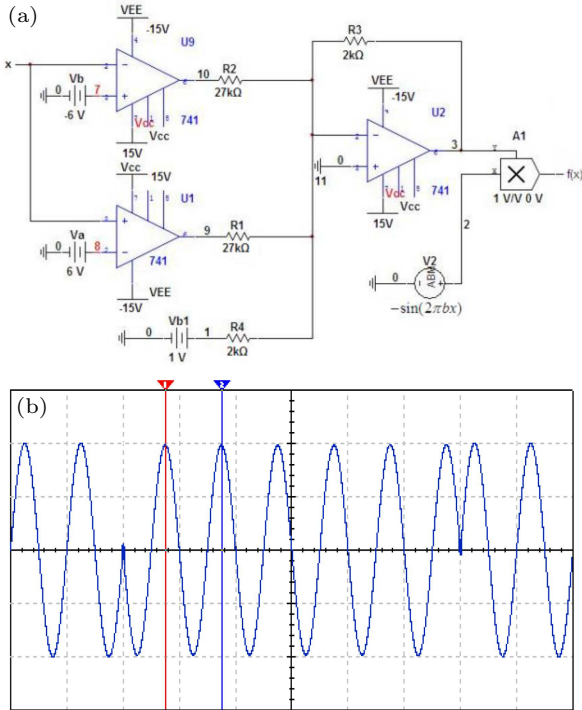


Fig. 6. The specific form of the sine function $f(x)$ with $b = 0.5$, $n_1 = n_2 = 3$. (a) Electronic circuit diagram; (b) simulation result with the unit of horizontal ordinate 2 s/Div, and the unit of vertical ordinate 500 mV/Div.

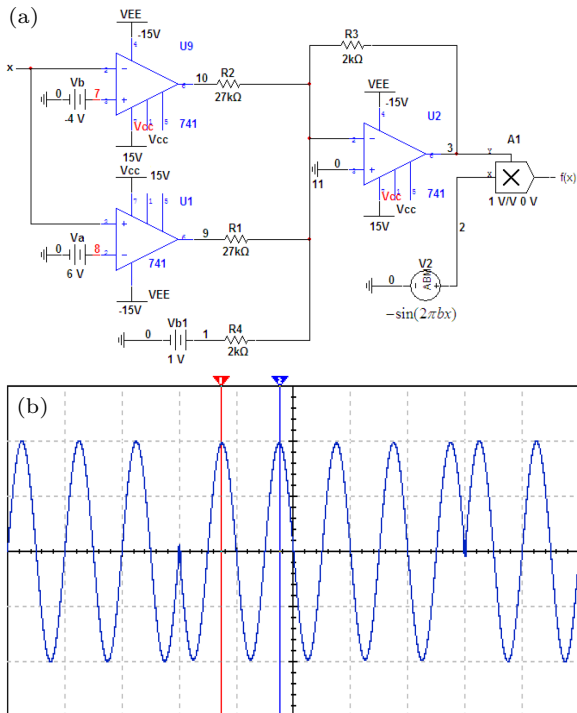


Fig. 7. The specific form of the sine function $f(x)$ with $b = 0.5$, $n_1 = 2$, $n_2 = 3$. (a) Electronic circuit diagram; (b) simulation result with the unit of horizontal ordinate 2 s/Div, and the unit of vertical ordinate 500 mV/Div.

4.2. Circuit design for the sign function generator

According to Eq. (10) with $A = 1$ and $M = 1$, the circuit for the sign function is designed and the circuit simulation result is shown in Fig. 8. The unit of horizontal ordinate is 1 V/Div, while the unit of vertical ordinate is 2 V/Div in Fig. 8(b). In Fig. 8(a), the resistance is selected as $R_3 = 2\text{ k}\Omega$, $R_1 = R_2 = 27\text{ k}\Omega$, and the operational amplifiers are uA741.

Based on Eq. (11) with $A = 1$ and $M = 2$, the circuit for sign function (11) is designed and the simulation result is shown in Fig. 9. The unit of horizontal ordinate is 1 V/Div, while the unit of vertical ordinate is 2 V/Div in Fig. 9(b).

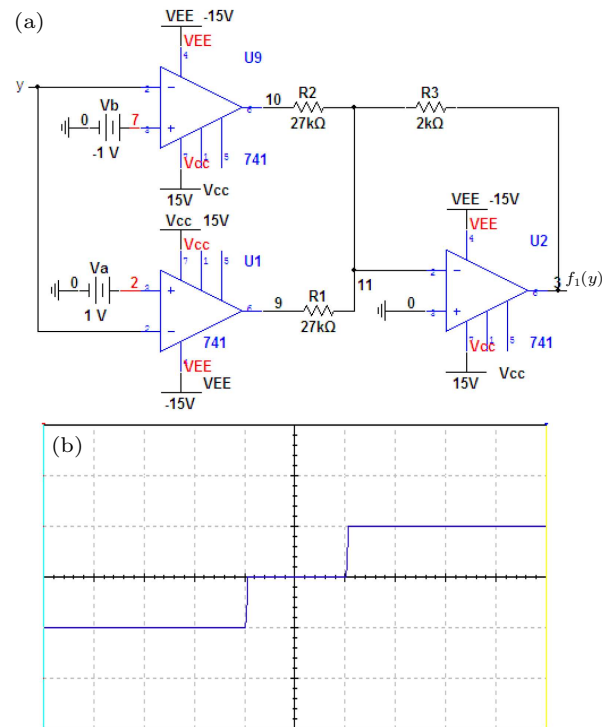


Fig. 8. The sign function $f_1(y)$ of Eq. (10) with $A = 1$, $M = 1$. (a) Electronic circuit diagram; (b) circuit simulation result with the unit of horizontal ordinate 1 V/Div, and the unit of vertical ordinate 1 V/Div.

4.3. Circuit design of the grid multi-scroll chaotic attractor

To verify the theoretical analysis, the circuit for the grid multi-scroll chaotic attractor is designed according to the chaotic system (9), which is shown in Fig. 10. This circuit consists of amplifiers uA741, analog multipliers ad633, resistors, and capacitances. When the signal $f(x)$ in Fig. 6(a) and $f_1(y)$ in Fig. 8(a) are connected to the input port $f(x)$ and $f_1(y)$ in Fig. 10, respectively, then the circuit of Fig. 10 can generate 6×3 grid multi-scroll chaotic attractors, which is shown in Fig. 11(a). Moreover, when the signal $f(x)$ in Fig. 7(a) and $f_1(y)$ in Fig. 9(a) are connected to the input port $f(x)$ and $f_1(y)$ in Fig. 10, respectively, the 5×4 grid multi-scroll chaotic attractor can be generated, which is displayed in Fig. 11(b).

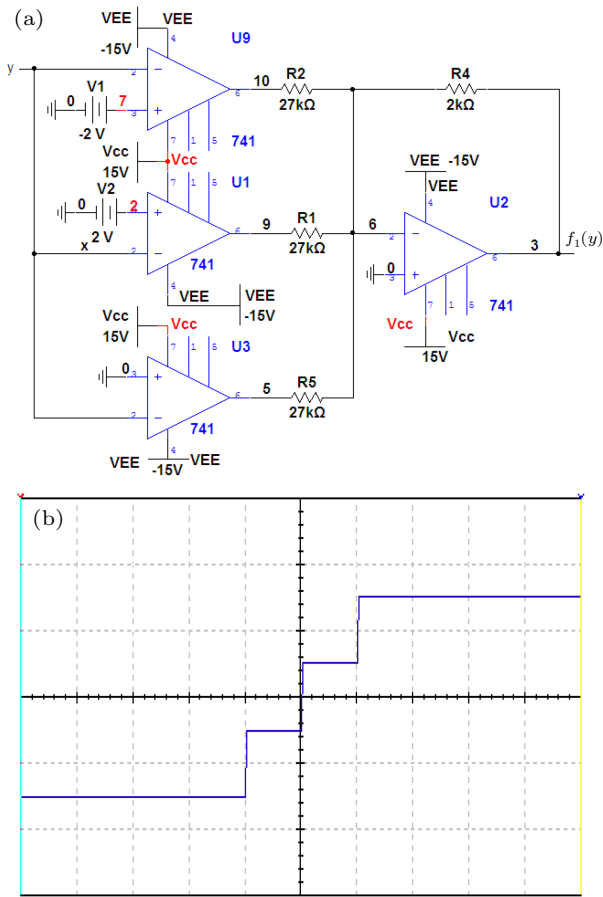


Fig. 9. The sign function $f_1(y)$ of Eq. (11) with $A = 1, M = 1$. (a) Electronic circuit diagram; (b) circuit simulation result with the unit of horizontal ordinate 1 V/Div, and the unit of vertical ordinate 2 V/Div.

According to circuit theory, the circuit equation of the circuit in Fig. 10 can be obtained as follows:

$$\begin{cases} R_4 C_1 \frac{dX}{dt} = \frac{R_3}{R_{27}} (-f_1(y)) + \frac{R_3}{R_{27}} Y, \\ R_{10} C_2 \frac{dY}{dt} = \frac{R_9}{R_8} Z, \\ R_{14} C_3 \frac{dZ}{dt} = \frac{R_{13}}{R_6} (-f(x)) + \frac{R_{13}}{R_{12}} (-y - f_1(y)) \\ \quad + \frac{R_{13}}{R_{11}} \left(-\frac{R_{16}}{R_{15}} Z \right). \end{cases} \quad (24)$$

In order to satisfy Eq. (9) with the parameters of $a = 1, c = 0.3, d = 0.5$, the values of resistors and capacitances are set as in Fig. 10. The circuit simulation results of the 6×3 grid multi-scroll chaotic attractor and the 5×4 grid multi-scroll chaotic attractor are shown in Fig. 11. From Figs. 3 and 11, it can be seen that the circuit simulation results are similar to the numerical simulation results.

Based on the circuits of the specific form of the sine function generator in Figs. 6 and 7, the circuits of the sign function generator in Figs. 8 and 9, and the grid multi-scroll chaotic attractor circuit in Fig. 10, the hardware circuits are designed and implemented. The electronic components are se-

lected as shown in Figs. 6–10. In Figs. 6 and 7, the sine function of $-\sin(2\pi bx)$ is realized based on the microprocessor of STM32F103. The hardware circuits experimental results are shown in Fig. 12.

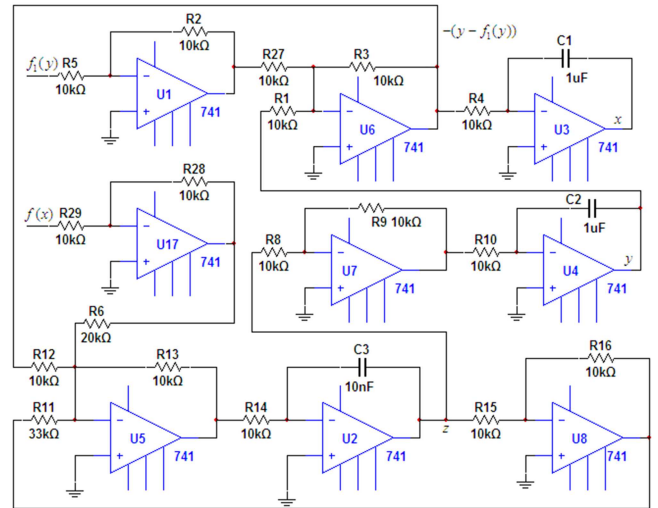


Fig. 10. Grid multi-scroll chaotic attractor circuit.

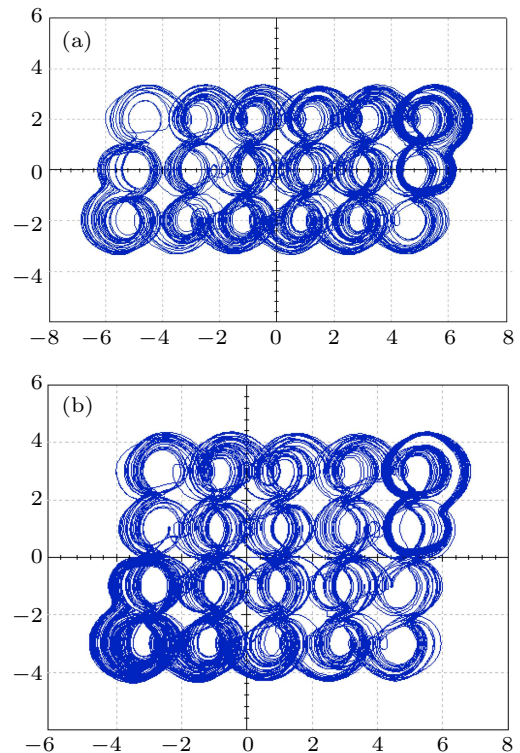


Fig. 11. Circuit simulation results: (a) 6×3 grid multi-scroll chaotic attractors, (b) 5×4 grid multi-scroll chaotic attractors.

From Fig. 12, the occurrence of the 6×3 grid multi-scroll chaotic attractors and the 5×4 grid multi-scroll chaotic attractors can be clearly seen. By comparing Fig. 12 with Fig. 11, it can be concluded that the generated chaotic attractors by the hardware circuits are similar to the ones in Fig. 11.

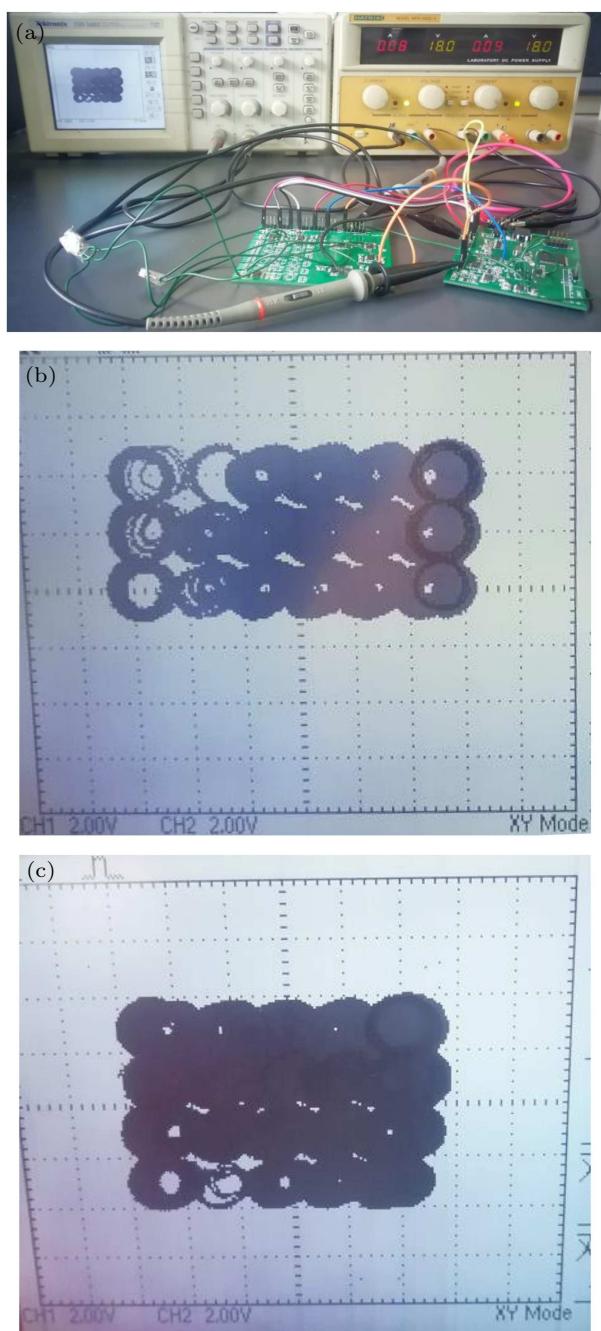


Fig. 12. Hardware circuits experimental results. (a) Hardware circuits connection diagram; (b) experimental results of the 6×3 grid multi-scroll chaotic attractors; (c) experimental results of the 5×4 grid multi-scroll chaotic attractors.

5. Conclusion and perspectives

In this paper, we have introduced novel 2D grid multi-scroll chaotic attractors based on the Jerk system. The novel chaotic attractor is constructed by introducing a specific form of sine function and a sign function series to increase the saddle points of index 2. The scroll numbers in the positive axis and the negative axis of the x -direction can be controlled independently and adjusted arbitrarily. Furthermore, the implementation of the circuit of the grid multi-scroll chaotic attractors needs only changing the threshold voltages of the specific form of the sine function generator for modifying the number

of scrolls in the x -direction. In contrast to triangular wave, saturation function, step function, hysteresis function, and piecewise linear function, the specific form of the sine function non-linearity in circuit realization has no need to change the structure of the circuit, and the circuit realization is simpler. The numerical simulation results and electronic circuit simulation results are in good agreement with each other. What is more, the other novel multi-scroll chaotic attractors with simple circuit realization can be easily obtained by using this specific form of the sine function.

References

- [1] Wang G Y and He S L 2003 *IEEE Transactions on Circuits and Systems-I: Fundamental Theory & Applications* **50** 945
- [2] Xiang X Q and Shi B C 2010 *Chaos* **20** 013104
- [3] Jin T and Zhang H 2011 *Science China-Information Sciences* **54** 2324
- [4] Ma S S, Lu M, Ding J F, Huang W and Yuan H 2015 *Science China-Information Sciences* **58** 102401
- [5] Kacar S 2016 *Optik* **127** 9551
- [6] Vaidyanathan S, Akgul A, Kacar S and Cavusoglu U 2018 *Euro. Phys. J. P.* **133** 46
- [7] Jiang Y J and Tang S Y 2018 *Multimedia Systems* **24** 355
- [8] Xiong Z L, Qu S C and Luo J 2019 *Complexity* **2019** 3827201
- [9] Liu J X, Wang Z X, Shu M L, Zhang F F, Leng S and Sun X H 2019 *Complexity* **2019** 7242791
- [10] Yu F, Zhang Z N, Liu L, Shen H, Huang Y Y, Shi C Q, Cai S, Song Y, Du S C and Xu Q 2020 *Complexity* **2020** 5859273
- [11] Chang D, Li Z J, Wang M J and Zeng Y C 2018 *Aeu-International Journal of Electronics and Communications* **88** 20
- [12] Liu L Z, Zhang J Q, Xu G X, Liang L S and Wang M S 2014 *Acta Phys. Sin.* **63** 010501 (in Chinese)
- [13] Yu F, Qian S, Chen X, Liu L, Shi C Q, Cai S, Song Y and Wang C H 2020 *International Journal of Bifurcation and Chaos* **2020**
- [14] Xie E Y, Li C Q, Yu S M and Lü J H 2017 *Signal Processing* **132** 150
- [15] Zhang L M, Sun K H, Liu W H and He S B 2017 *Chin. Phys. B* **26** 100504
- [16] Liu Z Y, Xia T C and Wang J B 2018 *Chin. Phys. B* **27** 030502
- [17] Asgari-Chenaghlu M, Balafar M-A and Feizi-Derakhshi M R 2019 *Signal Processing* **157** 1
- [18] Wang S C, Wang C H and Xu C 2019 *Optics and Lasers in Engineering* **128** 105995
- [19] Zhou M J and Wang C H 2020 *Signal Processing* **171** 107484
- [20] Xu C, Sun J R and Wang C H 2020 *International Journal of Bifurcation and Chaos* **30** 2050060
- [21] Lin H R and Wang C H 2020 *Applied Mathematics and Computation* **369** 124840
- [22] Lin H R, Wang C H and Tan Y M 2020 *Nonlinear Dynamics* **99** 2369
- [23] Yu F, Liu L, Qian S, Li L X, Huang Y Y, Shi C Q, Cai S, Wu X M, Du S C and Wan Q Z 2020 *Complexity* **2020** 8034196
- [24] Yu F, Liu L, He B Y, Huang Y Y, Shi C Q, Cai S, Song Y, Du S C and Wan Q Z 2019 *Complexity* **2019** 4047957
- [25] Jin J and Cui L 2019 *Complexity* 4106398
- [26] Yu F, Liu L, Shen H, Liu L, Zhang Z N, Huang Y Y, Shi C Q, Cai S, Wu X M, Du S C and Wang Q Z 2020 *Complexity* **2020** 5904607
- [27] Yu F, Shen H, Liu L, Zhang Z N, Huang Y Y, He B Y, Cai S, Song Y, Yin B, Du S C and Xu Q 2020 *Complexity* **2020** 5212601
- [28] Suykens J A K and Vandewalle J 1993 *IEEE Transactions on Circuits and Systems-I: Fundamental Theory and Applications* **40** 861
- [29] Zhong G Q, Man K F and Chen G R 2002 *International Journal of Bifurcation and Chaos* **12** 2907
- [30] Wang F Q and Liu C X 2007 *Chin. Phys.* **16** 942
- [31] Zhang C X and Yu S M 2009 *Chin. Phys. B* **18** 119
- [32] Sanchez-Lopez C 2011 *Applied Mathematics and Computation* **217** 4350
- [33] Dalia Pano-Azucena A, de Jesus Rangel-Magdaleno J, Tlelo-Cuautle E and de Jesus Quintas-Valles A 2017 *Nonlinear Dynamics* **87** 2203
- [34] Yalcin M E, Suykens J A K, Vandewalle J and Ozoguz S 2002 *International Journal of Bifurcation and Chaos* **12** 23

- [35] Lü J H, Chen G R, Yu X H and Leung H 2004 *IEEE Transactions on Circuits and Systems-I: Regular Papers* **51** 2476
- [36] Zhang G T and Wang F Q 2018 *Chin. Phys. B* **27** 018201
- [37] Chen S B, Zeng Y C, Xu M L and Chen J S 2011 *Acta Phys. Sin.* **60** 020507 (in Chinese)
- [38] Zhang C X and Yu S M 2016 *Chin. Phys. B* **25** 050503
- [39] Li C L, Yu S M and Luo X S 2012 *Acta Phys. Sin.* **61** 110502 (in Chinese)
- [40] Zhang X, Wang C H, Yao W and Lin H R 2019 *Nonlinear Dynamics* **97** 2159
- [41] Zhang X and Wang C H 2019 *International Journal of Bifurcation and Chaos* **29** 1950117
- [42] Zhang X and Wang C H 2019 *IEEE Access* **7** 16336
- [43] Deng Q L and Wang C H 2019 *Chaos* **29** 093112
- [44] Ji Q B, Zhou Y, Yang Z Q and Meng X Y 2015 *Chin. Phys. Lett.* **32** 050501
- [45] Van Ha N and Song H J 2015 *Chin. Phys. Lett.* **32** 038201
- [46] Sato Y D 2013 *Chin. Phys. Lett.* **30** 128201
- [47] Zhou J C and Song H J 2013 *Chin. Phys. Lett.* **30** 020501
- [48] Nam S G, Nguyen Van H and Song H J 2014 *Chin. Phys. Lett.* **31** 060502
- [49] Van Ha N and Song H J 2013 *Chin. Phys. Lett.* **30** 060501
- [50] Li X H and Bi Q S 2013 *Chin. Phys. Lett.* **30** 070503
- [51] Niu S, Shuai J W and Qi H 2017 *Acta Phys. Sin.* **66** 238701 (in Chinese)
- [52] Zhang H, Guo X X and Xiang S Y 2018 *Acta Phys. Sin.* **67** 204202 (in Chinese)
- [53] Li H M, Fan Y Y, Sun H Y, Zhang J and Jia M 2012 *Acta Phys. Sin.* **61** 029501 (in Chinese)
- [54] Zhang R, Peng M, Zhang Z D and Bi Q S 2018 *Chin. Phys. B* **27** 110501
- [55] Han Q S, Chen D Y and Zhang H 2017 *Chin. Phys. B* **26** 128202
- [56] Zhang L, Tang J S and Han Q 2018 *Chin. Phys. B* **27** 094702
- [57] Wang D G, Zhou C H and Zhang X P 2017 *Chin. Phys. B* **26** 128709
- [58] Gao X, Chen D Y, Zhang H, Xu B B and Wang X Y 2018 *Chin. Phys. B* **27** 128202
- [59] Dong L F, Yue H, Fan W L, Li Y Y, Yang Y J and Xiao H 2011 *Acta Phys. Sin.* **60** 065206 (in Chinese)
- [60] Dong L F, Li S F and Fan W L 2011 *Acta Phys. Sin.* **60** 065205 (in Chinese)
- [61] Wang F Q and Liu C X 2006 *Chin. Phys.* **15** 2878
- [62] Chen L, Shi Y D and Wang D S 2010 *Chin. Phys. B* **19** 100503
- [63] Luo X H, Tu Z W, Liu X R, Cai C, Liang Y L and Gong P 2010 *Chin. Phys. B* **19** 070510
- [64] Yalcin M E 2007 *Chaos Solitons Fract.* **34** 1659
- [65] Wang C H, Luo X W and Wan Z 2014 *Optik* **125** 6716
- [66] Ai W, Sun K H and Fu Y L 2018 *International Journal of Modern Physics C* **29** 1850049
- [67] Ma J, Wu X Y, Chu R T and Zhang L P 2014 *Nonlinear Dynamics* **76** 1951
- [68] Zhang J X and Tang W S 2009 *Chaos Solitons & Fractals* **42** 2181
- [69] He S B, Sun K H, Wang H H, Ai X X and Xu Y X 2016 *Journal of Applied Analysis and Computation* **6** 1180
- [70] Yu S M, Lü J H, Leung H and Chen G R 2005 *IEEE Transactions on Circuits and Systems-I: Regular Papers* **52** 1459
- [71] Tang W K S, Zhong G Q, Chen G R and Man K F 2001 *IEEE Transactions on Circuits and Systems-I: Fundamental Theory and Applications* **48** 1369
- [72] Luo X H 2009 *Chin. Phys. B* **18** 3304
- [73] Hadeif S and Boukabou A 2014 *Journal of the Franklin Institute-Engineering and Applied Mathematics* **351** 2728
- [74] Li F and Ma J 2016 *Plos One* **11** e0154282
- [75] Hu X Y, Liu C X, Liu L, Ni J K and Li S L 2016 *Nonlinear Dynamics* **86** 1725
- [76] Hu X Y, Liu C X, Liu L, Yao Y P and Zheng G C 2017 *Chin. Phys. B* **26** 110502